

Quantum-enhanced optical precision measurement assisted by low-frequency squeezed vacuum states

Guohui Kang(康国辉), Jinxia Feng(冯晋霞), Lin Cheng(程琳),Yuanji Li(李渊骥), and Kuanshou Zhang(张宽收)
Citation: Chin. Phys. B, 2023, 32 (**10**): 104204. DOI: 10.1088/1674-1056/acc520
Journal homepage: http://cpb.iphy.ac.cn; http://iopscience.iop.org/cpb

What follows is a list of articles you may be interested in

Principle of subtraction ghost imaging in scattering medium

Qin Fu(付芹), Yanfeng Bai(白艳锋), Wei Tan(谭威), Xianwei Huang(黄贤伟), Suqin Nan(南苏琴), and Xiquan Fu(傅喜泉)
Chin. Phys. B, 2023, 32 (**6**): 064203. DOI: 10.1088/1674-1056/acb202

Tunable magnomechanically induced transparency and fast-slow light in a hybrid cavity magnomechanical system

Qinghong Liao(廖庆洪), Kun Peng(彭坤), and Haiyan Qiu(邱海燕)
Chin. Phys. B, 2023, 32 (**5**): 054205. DOI: 10.1088/1674-1056/acaf2b

Quantum optical interferometry via general photon-subtracted two-mode squeezed states

Li-Li Hou(侯丽丽), Jian-Zhong Xue(薛建忠), Yong-Xing Sui(眭永兴), Shuai Wang(王帅)
Chin. Phys. B, 2019, 28 (**9**): 094217. DOI: 10.1088/1674-1056/ab38a9

Generation of squeezed vacuum on cesium D2 line down to kilohertz range

Jian-Feng Tian(田剑锋), Guan-Hua Zuo(左冠华), Yu-Chi Zhang(张玉驰), Gang Li(李刚), Peng-Fei Zhang(张鹏飞), Tian-Cai Zhang(张天才)
Chin. Phys. B, 2017, 26 (**12**): 124206. DOI: 10.1088/1674-1056/26/12/124206

Phase estimation of phase shifts in two arms for an SU(1,1) interferometer with coherent and squeezed vacuum states

Qian-Kun Gong(龚乾坤), Dong Li(李栋), Chun-Hua Yuan(袁春华), Ze-Yu Qu(区泽宇), Wei-Ping Zhang(张卫平)
Chin. Phys. B, 2017, 26 (**9**): 094205. DOI: 10.1088/1674-1056/26/9/094205

Quantum-enhanced optical precision measurement assisted by low-frequency squeezed vacuum states

Guohui Kang(康国辉)[1], Jinxia Feng(冯晋霞)[1,2,†], Lin Cheng(程琳)[1], Yuanji Li(李渊骥)[1,2], and Kuanshou Zhang(张宽收)[1,2]

[1] *State Key Laboratory of Quantum Optics and Quantum Optics Devices, Institute of Opto-Electronics, Shanxi University, Taiyuan* 030006, *China*
[2] *Collaborative Innovation Center of Extreme Optics, Shanxi University, Taiyuan* 030006, *China*

(Received 14 November 2022; revised manuscript received 13 February 2023; accepted manuscript online 17 March 2023)

Stable low-frequency squeezed vacuum states at a wavelength of 1550 nm were generated. By controlling the squeezing angle of the squeezed vacuum states, two types of low-frequency quadrature-phase squeezed vacuum states and quadrature-amplitude squeezed vacuum states were obtained using one setup respectively. A quantum-enhanced fiber Mach–Zehnder interferometer (FMZI) was demonstrated for low-frequency phase measurement using the generated quadrature-phase squeezed vacuum states that were injected. When phase modulation was measured with the quantum-enhanced FMZI, there were above 3 dB quantum improvements beyond the shot-noise limit (SNL) from 40 kHz to 200 kHz, and 2.3 dB quantum improvement beyond the SNL at 20 kHz was obtained. The generated quadrature-amplitude squeezed vacuum state was applied to perform low-frequency amplitude modulation measurement for sensitivity beyond the SNL based on optical fiber construction. There were about 2 dB quantum improvements beyond the SNL from 60 kHz to 200 kHz. The current scheme proves that quantum-enhanced fiber-based sensors are feasible and have potential applications in high-precision measurements based on fiber, particularly in the low-frequency range.

Keywords: squeezed vacuum states, fiber Mach–Zehnder interferometer, optical precision measurement

PACS: 42.50.–p, 42.50.Dv **DOI:** 10.1088/1674-1056/acc520

Optical precision measurement based on optical interferometers is an important metrology technique that performs with high sensitivity. Its sensitivity is ultimately limited by the quantum fluctuation noise of the light field, which leads to a shot-noise limit (SNL).[1,2] Squeezed states of light can be used to improve the sensitivity of the precision measurement of a physical parameter, because the noise of the quadrature component of squeezed states is lower than that of coherent states.[3–10] In 1981, Caves envisaged that the vacuum field can be replaced with quadrature phase squeezed vacuum states to enter the interferometer, thereby realizing measurements beyond the SNL.[3] Subsequently, phase modulation measurement beyond the SNL in a laser interferometer was demonstrated experimentally.[4] Squeezing-enhanced optical precision measurement has been made available for many areas, such as amplitude modulation measurement,[5] small displacement measurement,[6] optical magnetometry,[7] dynamic biologic measurement,[8] phase estimation and tracking.[9,10] In the above applications, the frequencies of the measured signal were almost in the MHz range. However, the signal with frequencies in the kHz regime needs to be measured in many optical precision measurements, such as general position and strain measurement, and gravitational wave (GW) detection. Due to the fact that there are complicated and various noises at low frequency, the generation of squeezed vacuum states at low frequency is a great challenge.[11–18] Recently, several key techniques, including a coherent control scheme,[13] the optical serrodyne sideband modulation locking method,[14] and the audio frequency balanced homodyne detection method,[15] have been developed and used to generate low-frequency squeezed vacuum states at a wavelength of 1064 nm in the kHz regime, and even in a broad Fourier frequency band down to 1 Hz.[16] The low-frequency squeezed vacuum states at a wavelength of 1064 nm were used to increase the sensitivity of GW detectors.[13,15–18] Moreover, low-frequency squeezed vacuum states can be potentially used in optical fiber sensors based on fiber interferometers. Optical fiber sensors, which have the advantages of high sensitivity, compact size, low cost and suitability for many types of environments,[19,20] can be applied to the sensing of strain, sound and spectrometer absorption.[21,22] A squeezing-enhanced fiber interferometer was demonstrated to measure a low-frequency phase modulated signal using the high-frequency (MHz range) sidebands of squeezed vacuum states at 1064 nm.[23] However, stable low-frequency squeezed vacuum states at 1550 nm are an optimal choice for a squeezing-enhanced fiber interferometer. So far, squeezed vacuum states at 1550 nm have been generated by several groups,[24–28] but the analysis frequencies of the generated squeezed vacuum states were in the MHz range. Recently, squeezed vacuum states at 1550 nm at frequencies from 10 kHz down to below 1 Hz with a quantum noise reduction of up to 11.5 dB were investigated.[29] The squeezing angle of the squeezed vacuum states was not controlled, and an arbitrarily orthogonal component squeezed vacuum state was obtained.

†Corresponding author. E-mail: fengjx@sxu.eud.cn

© 2023 Chinese Physical Society and IOP Publishing Ltd

In this paper, stable low-frequency squeezed vacuum states at a wavelength of 1550 nm were generated from a subthreshold triply resonant optical parametric oscillator (OPO). By controlling the squeezing angle of the squeezed vacuum states, two types of low-frequency quadrature-phase squeezed vacuum states and quadrature-amplitude squeezed vacuum states were obtained using one setup, respectively. The squeezing angle of the squeezed vacuum states was controlled by a coherent control technique using a fundamental laser whose frequency was shifted by two acousto-optic modulators (AOMs). Its applications of two types of low-frequency quadrature-phase squeezed vacuum states and quadrature-amplitude squeezed vacuum states to quantum-enhanced optical precision measurement were further investigated. By employing a squeezing-enhanced fibers framework, the low-frequency phase and amplitude modulated signals were measured beyond the SNL using the generated low-frequency quadrature-phase squeezed vacuum states and quadrature-amplitude squeezed vacuum states.

A schematic of the experimental setup for generation of low-frequency squeezed vacuum states at 1550 nm is shown in Fig. 1(a). A commercial fiber laser (NP Photonic Inc.) provided an output power of 2.0 W with continuous-wave (CW) single-frequency operation at 1550 nm. The laser beam was sent through a mode clear (MC1) with a finesse of 500 and linewidth of 600 kHz for preliminary filtering of the laser spatial mode and excess intensity noise. The output from MC1 was split into three parts. A small part of the 1550 nm laser was sent through MC2 with a linewidth of 600 kHz to reduce the excess intensity noise further, and the output from MC2 acted as a local oscillator (LO) and probe beams for the next measurement experiments. The main portion was injected into an external enhanced second harmonic generation (SHG) cavity to obtain a high-power low-noise 775 nm CW laser. The 775 nm laser with the excess intensity noises reduced by MC3 with a linewidth of 700 kHz further and power stabilized by a power stabilization system based on a Mach–Zehnder Interferometer (MZI) was employed as the pump of the OPO. The OPO was a semi-monolithic cavity composed of a type-I phase-matched periodically poled potassium titanyl phosphate (PPKTP) crystal with dimensions of 1 mm × 2 mm × 10 mm and a concave mirror with a radius of 30 mm. The concave face of the concave mirror that acted as input and output couplers was partially transmission coated at 1550 nm and 775 nm ($T_{1550\ \mathrm{nm}} = 13\%$ & $T_{775\ \mathrm{nm}} = 5.6\%$). The flat face of the concave mirror was antireflection (AR) coated at 1550 nm and 775 nm ($R_{1550\ \mathrm{nm\&775\ nm}} < 0.1\%$). One end of the PPKTP crystal was a convex surface with a radius of 12 mm and HR coated at 1550 nm and 775 nm ($R_{1550\ \mathrm{nm\&775\ nm}} > 99.9\%$). Another end of the PPKTP crystal was a flat surface and AR coated at 1550 nm ($R_{1550\ \mathrm{nm\&775\ nm}} < 0.1\%$) and at 775 nm ($R_{775\ \mathrm{nm}} < 0.25\%$).

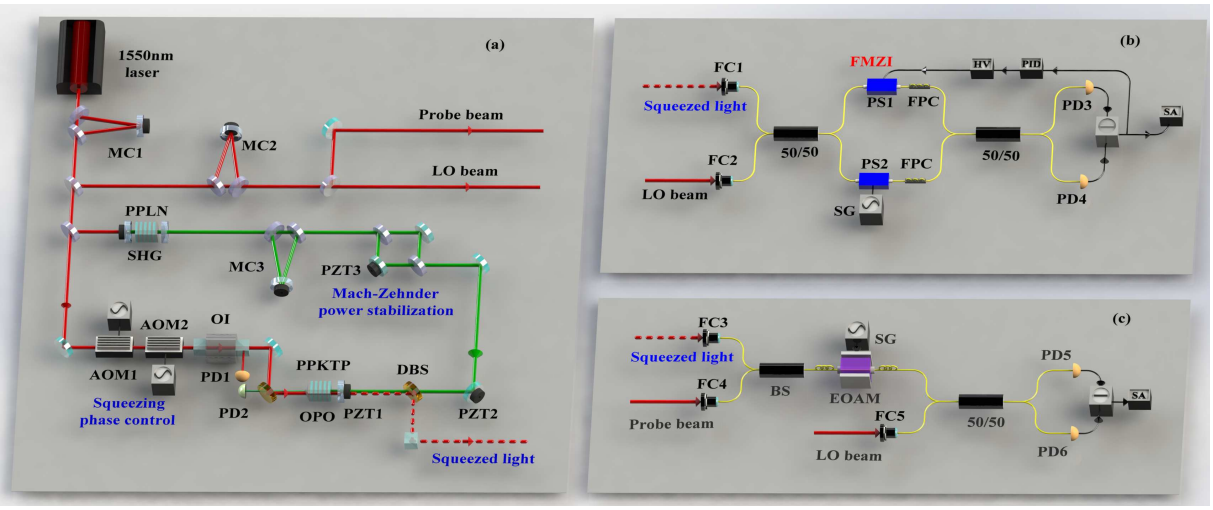


Fig. 1. A schematic of the experimental setup used to generate stable low-frequency squeezed vacuum states at a wavelength of 1550 nm. MC1-2: mode cleaner of 1550 nm; SHG: second harmonic generator; MC3: mode cleaner of 775 nm; AOM1-2: acousto-optic modulator; OI: optical isolator; PZT1-3: piezo-electric transducer; DBS: dichroic beam splitter; OPO: optical parametric oscillator; PD1-6: photodetector; BS1-4: fiber beam splitter; FC1-5: fiber coupler; PS1-2: fiber phase shifter; EOAM: electro-optical amplitude modulator; FPC: fiber polarization controllers; ⊖: negative power combiner; PID: proportional-integral-derivative; HV: high-voltage amplifier; SA: spectrum analyzer.

The pump, signal, and idler were resonant simultaneously in the OPO cavity. The signal and idler were degenerating on both the frequency and polarization. The PPKTP crystal was housed in a copper oven and temperature controlled by a homemade temperature controller with an accuracy of 0.01 °C. The temperature of the PPKTP was controlled at 35.8 °C to realize optimum phase matching. The concave mirror was mounted on a piezo-electric transducer (PZT1) and the length of the OPO cavity was controlled by PZT1. The length of the OPO cavity was 35 mm, which leads to a linewidth of 65 MHz. When the OPO was subthreshold operated, squeezed vacuum states were generated experimentally. The third portion of the

1550 nm laser from MC1 was frequency shifted by two AOMs and acted as an auxiliary beam that was used to control the squeezing angle of the generated squeezed vacuum states.

When the auxiliary beam was injected into the OPO, a second sideband was produced via difference frequency generation. An optical isolator (OI) was applied to extract the reflected light. The auxiliary beam reflected from the OPO was detected by a photodiode (PD1). The error signal was obtained by demodulating the photocurrent from PD1 using a sinusoidal signal. It was used to feed back to the PZT2 to lock the relative phase between the pump and auxiliary beam, i.e., to control or lock the squeezing angle of the generated squeezed vacuum states. Squeezed vacuum states at a wavelength of 1550 nm in an arbitrary quadrature can be generated by controlling the squeezing angle. The auxiliary beam was used to control the squeezing angle, and the frequency of the auxiliary beam was shifted out of the squeezing band to prevent contamination of the squeezed field in the low-frequency range. As a result, stable low-frequency squeezed vacuum states at a wavelength of 1550 nm were generated.

The threshold of the triply resonant OPO was measured first; the squeezed vacuum states are generated by a subthreshold OPO.[30] The measured threshold was 28 mW. When 775 nm pump power was 22 mW, the OPO was operated below the threshold. The length of the OPO cavity was locked using the Pound–Drever–Hall (PDH) technique. The transmission of the pump from the OPO was detected by PD2. Meanwhile, the auxiliary beam with a power of 100 μW was injected into the subthreshold OPO. The auxiliary beam was generated by a frequency-shifting 1550 nm laser with a frequency of 25 MHz. The first AOM was used to shift the frequency of the 1550 nm laser beam by 200 MHz and the second was used to shift the frequency of the beam by −175 MHz. A sinusoidal signal with frequency of 50 MHz was used to demodulate the photocurrent from PD1 and then obtain the error signal. When the relative phase between the pump and auxiliary beam was locked to 0 ($\pi/2$), quadrature-phase (quadrature-amplitude) squeezed vacuum states were achieved. Furthermore, squeezed vacuum states in an arbitrary quadrature can be generated by controlling the value of the relative phase between the pump and auxiliary beam from 0 to π. A balanced homodyne detector (BHD) system was employed to measure the noise power of the squeezed vacuum field from the subthreshold OPO. The squeezed field and LO were combined by a 50/50 beam splitter (BS) and were detected by a pair of InGaAs photodiodes with a quantum efficiency of $\eta_{\rm qe} = 92\%$. The homodyne efficiency is defined by $\zeta = \eta_{\rm qe}\eta_{\rm P}\eta_{\rm V}^2$. Here, $\eta_{\rm P}$ is the propagation efficiency of optical components, with a measured value of 98.6%, and $\eta_{\rm V}$ is the homodyne visibility of 98.8%. The homodyne efficiency is 88.5%. A clearance of 20 dB between the SNL and the electronic noise can be achieved when the amplifier is illuminated by a 60 μW laser. When the relative phase between the auxiliary beam and LO is $\pi/2$ (0), the generated quadrature-phase (quadrature-amplitude) squeezed vacuum states can be measured continuously.

Figure 2 shows the measured noise power of squeezed vacuum states at a Fourier frequency of 1 kHz–200 kHz recorded by an SA with a resolution bandwidth (RBW) of 200 Hz, a video bandwidth (VBW) of 10 Hz and a sweep time of 1 second. The curves (i) in Fig. 2 are the SNL, which was calibrated using a thermal field. The curves (ii) in Figs. 2(a) and 2(b) are the measured squeezing noise of the quadrature-phase and quadrature-amplitude squeezed vacuum states, respectively. The curves (iii) in Figs. 2(a) and 2(b) are the measured anti-squeezing noise of quadrature-phase and quadrature-amplitude squeezed vacuum states, respectively. It can be seen that the measured squeezing degrees of the quadrature-phase and quadrature-amplitude squeezed vacuum states from 40 kHz to 200 kHz are approximately 5.2 ± 0.5 dB and 5.0 ± 0.5 dB, respectively. When considering the homodyne efficiency of 88.5%, the actual output squeezing degrees are 6.8 dB and 6.4 dB, respectively. The measured squeezing degree of squeezed vacuum states decreases with the decrease of frequency within the 6 kHz to 40 kHz regime. Here, 2.7 ± 0.5 dB quadrature-phase and quadrature-amplitude squeezed vacuum states were obtained at an audio frequency of 6 kHz, respectively. When considering the homodyne efficiency, the actual output squeezing degree of the quadrature-phase and quadrature-amplitude squeezed vacuum states is 3.2 dB. The generated quadrature-phase squeezed vacuum state was applied to a quantum-enhanced fiber Mach–Zehnder interferometer (FMZI) for low-frequency phase measurement, as shown in Fig. 1(b). The FMZI was constructed with two 2×2 single-mode polarization-maintaining fiber BS with a split ratio of 50:50 and two single-mode polarization-maintaining fibers with length of 10 m. The total loss of the system is about 28%. Fiber polarization controllers (FPCs) were used to maintain the polarization of the light fields in the FMZI. The generated quadrature-phase squeezed vacuum state and LO beam were coupled into the input ports of the FMZI by the fiber couplers (FC1 and FC2), respectively. A phase shifter (PS1) was used to control the relative phase between two light fields transmitted in two arms of the FMZI. A phase modulation signal, was loaded to PS2 by a signal generator (SG), which acted as a small phase variety to be measured by the FMZI. The noise power spectra of the output from the FMZI were measured by a BHD system that included PD3 and PD4. The subtraction of direct currents of photocurrents from PD3 and PD4 was used as the error signal and fed back to PS1 to lock the relative phase between the light fields of two arms in the FMZI. The alternating current part of the photocurrent subtraction was recorded by a spectrum analyzer (SA).

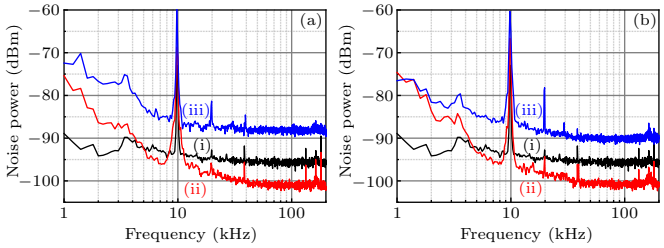


Fig. 2. Measured noise power of the squeezed vacuum states at a Fourier frequency of 1 kHz–200 kHz. The parameters of the SA: RBW of 30 Hz, VBW of 100 Hz and sweep time of 1 s. (a) The measured noise power of quadrature-phase squeezed vacuum states. (b) The measured noise power of quadrature-amplitude squeezed vacuum states. Curve (i): SNL. Curve (ii): squeezing noise. Curve (iii): anti-squeezing noise.

The phase measurement results at a low frequency of 20 kHz are displayed using the general and quantum-enhanced FMZI, respectively, as shown in Fig. 3(a). The input power of the LO was 60 μW, which yielded a dark noise clearance of 20 dB from 10 kHz to 1 MHz. A 20 kHz phase modulation signal was loaded to the PS2. Curve (i) shows a 100 kHz phase modulation measured with the general FMZI when the input port of the generated quadrature-phase squeezed vacuum state was blocked. Curve (ii) shows a 100 kHz phase modulation measured using the quantum-enhanced FMZI with 5.2 dB quadrature-phase squeezed vacuum state injection. Both noise power traces were normalized to the SNL. A 3.5 dB quantum improvement beyond the SNL at 100 kHz was obtained. Figure 3(b) shows the shot noise reduction when phase modulation was measured using the quantum-enhanced FMZI from 20 kHz to 200 kHz. More than 3 dB quantum improvements were obtained beyond the SNL from 40 kHz to 200 kHz. A 2.3 dB quantum improvement beyond the SNL at 20 kHz was obtained.

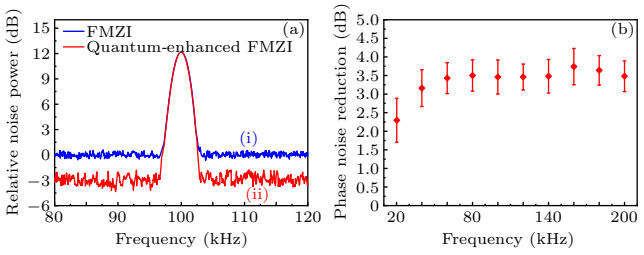


Fig. 3. (a) Phase modulation measurements for 20 kHz using the FMZI, where (i) is using the general FMZI, and (ii) is using the quantum-enhanced FMZI. (b) Shot noise reduction for measured phase modulation using the quantum-enhanced FMZI for low frequency (from 20 kHz to 200 kHz, in steps of 20 kHz).

The measurement of small changes in the amplitude of the electromagnetic field is of fundamental and practical importance in optical physics. The generated quadrature-amplitude squeezed vacuum state was applied to perform low-frequency amplitude modulation measurement for sensitivity beyond the SNL based on optical fiber construction, as shown in Fig. 1(c). The generated quadrature-amplitude squeezed vacuum state and a probe beam were coupled with a 2×1 single-mode polarization-maintaining fiber BS by the FC3 and FC4, respectively. The split ratio of the BS is 99:1. The weak probe beam and 99% of squeezed vacuum light were coupled into a fiber-based electro-optical amplitude modulator (EOAM) and modulated in amplitude at low frequency. The total loss of the system is about 35%. An amplitude modulation signal was loaded to the EOAM by an SG. The noise power spectra of the light fields output from the EOAM, called the signal fields, were measured by a BHD system that included PD5 and PD6. The alternating current part of the photocurrent subtraction was recorded by an SA.

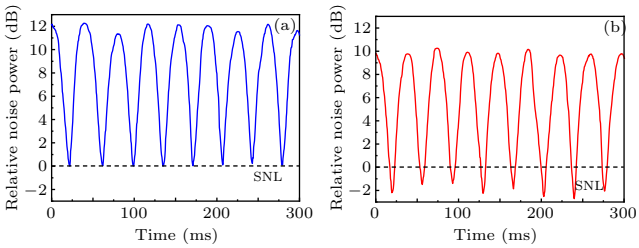


Fig. 4. The measured amplitude modulation signal when the relative phase between the LO and the signal fields was scanned (a) without the input of the generated quadrature-amplitude squeezed vacuum state, and (b) with the input of the generated quadrature-amplitude squeezed vacuum state.

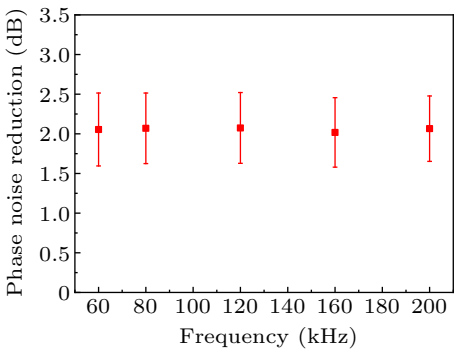


Fig. 5. Shot noise reduction for measured amplitude modulation using the quantum-enhanced fiber measurement device for low frequency (60 kHz, 80 kHz, 120 kHz, 160 kHz and 200 kHz).

The input powers of the probe and LO are 50 μW and 60 μW, respectively. A dark noise clearance is also about 20 dB from 10 kHz to 1 MHz. A 60 kHz amplitude modulation signal was loaded to the EOAM. Figure 4 shows the measured relative noise power spectra of photocurrent fluctuations. The dashed lines in Figs. 4(a) and 4(b) are the SNL, which were given when both the quadrature-amplitude squeezed vacuum state and probe beam were blocked. The solid curves in Figs. 4(a) and 4(b) show the measured amplitude modulation signal without and with the input of the generated quadrature-amplitude vacuum state when the relative phase between the LO and the signal fields was scanned. Both noise traces were normalized to the vacuum. The minimum level in Fig. 4(a) is the SNL. The maximum value is the noise power of the probe beam with the amplitude modulation signal at 60 kHz. A 2 dB reduction beyond the SNL for the measurement of the amplitude modulation signal is shown in Fig. 4(b) when the gen-

erated quadrature-amplitude squeezed vacuum state was injected. Figure 5 shows the shot noise reduction when the amplitude modulation signal was measured from 60 kHz, 80 kHz, 120 kHz, 160 kHz and 200 kHz. There are about 2 dB quantum improvements beyond the SNL from 60 kHz to 200 kHz.

In conclusion, we experimentally generated stable low-frequency squeezed vacuum states at a wavelength of 1550 nm. Due to the effective control of the squeezing angle, 5.2 ± 0.5 dB of quadrature-phase squeezed vacuum states and 5.0 ± 0.5 dB of quadrature-amplitude squeezed vacuum states from 40 kHz to 200 kHz were obtained using one setup, respectively. A 2.7 ± 0.5 dB quadrature-phase and quadrature-amplitude squeezed vacuum state was obtained at the audio frequency of 6 kHz. A quantum-enhanced FMZI was demonstrated for low-frequency phase measurement using the generated quadrature-phase squeezed vacuum states that were injected. When the phase modulation was measured with the quantum-enhanced FMZI, there were above 3 dB quantum improvements beyond the SNL from 40 kHz to 200 kHz, and 2.3 dB quantum improvement beyond the SNL at 20 kHz was obtained. The generated quadrature-amplitude squeezed vacuum state was applied to perform low-frequency amplitude modulation measurement for sensitivity beyond the SNL based on optical fiber construction. There are about 2 dB quantum improvements beyond the SNL from 60 kHz to 200 kHz. If the EOAM is replaced by a sample whose absorption is externally amplitude modulated, the fiber-based amplitude modulation measurement device can be regarded as a workable quantum-enhanced spectrometer. Our results show that quantum-enhanced fiber-based sensors are feasible, particularly in the low-frequency range.

Data availability statement

The data that support the findings of this study are openly available in Science Data Bank at the following link https://doi.org/10.57760/sciencedb.j00113.00094

Acknowledgments

Project supported by the National Natural Science Foundation of China (Grant No. 62175135) and the Fundamental Research Program of Shanxi Province (Grant No. 202103021224025).

References

[1] Caves C M, Thorne K S, Drever R W P, Sandberg V D and Zimmermann M 1980 *Rev. Mod. Phys.* **52** 341
[2] Braunstein S L and Loock P 2005 *Rev. Mod. Phys.* **77** 513
[3] Caves C M 1981 *Phys. Rev. D* **23** 1693
[4] Xiao M, Wu L A and Kimble H J 1987 *Phys. Rev. Lett.* **59** 278
[5] Xiao M, Wu L A and Kimble H J 1988 *Opt. Lett.* **13** 476
[6] Treps N, Grosse N, Bowen W P, Fabre C, Bachor H A and Lam P K 2003 *Science* **301** 940
[7] Wolfgramm F, Cere A, Beduini F A, Predojevic A, Koschorreck M and Mitchell M W 2010 *Phys. Rev. Lett.* **105** 053601
[8] Taylor M A, Janousek J, Daria V, Knittel J, Hage B, Bachor H A and Bowen W P 2013 *Nat. Photonics* **7** 229
[9] Berni A A, Gehring T, Nielsen B M, Händchen V, Paris M G A and Andersen U L 2015 *Nat. Photonics* **9** 577
[10] Yonezawa H, Nakane D, Wheatley T A, Iwasawa K, Takeda S, Arao H, Ohki K, Tsumura K, Berry D W, Ralph T C, Wiseman H M, Huntington E H and Furusawa A 2012 *Science* **337** 1514
[11] Bowen W P, Schnabel R, Treps N, Bachor H A and Lam P K 2002 *J. Opt. B* **4** 421
[12] McKenzie K, Grosse N, Bowen W P, Whitcomb S E, Gray M B, McClelland D E and Lam P K 2004 *Phys. Rev. Lett.* **93** 161105
[13] Vahlbruch H, Chelkowski S, Hage B, Franzen A, Danzmann K and Schnabel R 2006 *Phys. Rev. Lett.* **97** 011101
[14] Gao Y H, Feng J X, Li Y J and Zhang K S 2019 *Laser Phys. Lett.* **16** 055202
[15] Vahlbruch H, Khalaidovski A, Laszka N, Graf C, Danzmann K and Schnabel R 2010 *Class. Quantum Grav.* **27** 084027
[16] Vahlbruch H, Chelkowski S, Danzmann K and Schnabel R 2007 *New J. Phys.* **9** 371
[17] Oelker E, Isogai T, Miller J, Tse M, Barsotti L, Mavalvala N and Evans M 2016 *Phys. Rev. Lett.* **116** 041102
[18] Mehmet M and Vahlbruch H 2019 *Class. Quantum Grav.* **36** 015014
[19] Lee B 2003 *Opt. Fiber Technol.* **9** 57
[20] Tan W H, Shi Z Y, Smith S, Birnbaum D and Kopelman R 1992 *Science* **258** 778
[21] Gagliardi G, Salza M, Avino S, Ferraro P and De Natale P 2010 *Science* **330** 1081
[22] Shambat G, Kothapalli S R, Khurana A, Provine J, Sarmiento T, Cheng K, Cheng Z, Harris J, Daldrup-Link H, Gambhir S S and Vuckovic J 2012 *Appl. Phys. Lett.* **100** 213702
[23] Liu F, Zhou Y Y, Yu J, Guo J L, Wu Y, Xiao S X, Wei D, Zhang Y, Jia X J and Xiao M 2017 *Appl. Phys. Lett.* **110** 021106
[24] Feng J X, Tian X T, Li Y M and Zhang K S 2008 *Appl. Phys. Lett.* **92** 221102
[25] Mehmet M, Ast S, Eberle T, Steinlechner S, Vahlbruch H and Vahlbruch H 2011 *Opt. Express* **19** 25763
[26] Kaiser F, Fedrici B, Zavatta A, D'auria V and Tanzilli S 2016 *Optica* **3** 362
[27] Schonbeck S, Thies F and Schnabel R 2018 *Opt. Lett.* **43** 110
[28] Mehmet M and Vahlbruch H 2019 *Class. Quantum Grav.* **36** 015014
[29] Meylahn F, Willke B and Vahlbruch H 2022 *Phys. Rev. Lett.* **129** 121103
[30] Wu L A, Kimble H J, Hall J L and Wu H 1986 *Phys. Rev. Lett.* **57** 2520